

Received May 14, 2019, accepted July 7, 2019, date of publication July 10, 2019, date of current version July 29, 2019.

Digital Object Identifier 10.1109/ACCESS.2019.2927811

A Review of the Space Environment Effects on Spacecraft in Different Orbits

YIFAN LU^{ID}, QI SHAO, HONGHAO YUE, AND FEI YANG^{ID}

State Key Laboratory of Robotics and System, Harbin Institute of Technology, Harbin 150001, China

Corresponding author: Yifan Lu (yf.lu@hit.edu.cn)

This work was supported in part by the National Natural Science Foundation of China under Grant 51835002 and in part by the Self-Planned Task of State Key Laboratory of Robotics and System (HIT) under Grant SKLRS201808B.

ABSTRACT The space environment consists of various complex phenomena, which could have a strong influence on the spacecraft operation in different aspects. Since the very beginning of space exploration, numerous studies have been done on the space environment. However, most of the existing literature focuses on the investigation of the details of environmental phenomena, while the space environment has rarely been discussed from the perspective of orbits types. Therefore, a comprehensive review on analyzing and comparing the environmental characteristics among diverse orbits in space is of great significance. In this paper, the main components of the space environment are introduced, including the neutral atmosphere, the plasma environment, the radiation environment, the macroscopic particle environment, the geomagnetic field, the temperature field, and the solar activities. The relations of the various space environmental components are also discussed. The dominant environmental components and their effects on spacecraft in different orbits, i.e., the geosynchronous orbit (GEO), the low earth orbit (LEO), the medium earth orbit (MEO), and the high earth orbit (HEO), are investigated, respectively. The space environment that should be taken into particular consideration is summed up to facilitate the design of the spacecraft in a specific orbit.

INDEX TERMS Space environment, spacecraft design, geosynchronous orbit, low earth orbit, medium earth orbit, high earth orbit.

I. INTRODUCTION

More and more spacecraft are placed at different altitudes due to the momentous strategic position of space exploration. Generally speaking, the earth's space is divided into three regions. LEO is defined as the region from 160 km to 2000 km [1], which is the main affected zone of the upper atmosphere. MEO and HEO are separated by GEO which is at an altitude of 35786 km [2]. Table 1 shows the number of operating satellites in four types of orbits respectively according to the database producing by the Union of Concerned Scientists (UCS) [3]. It can be learnt that over half of the satellites are placed in LEO, and others are densely arranged in the vicinity of GEO. While MEO and the highly elliptical orbit have a few satellites by contrast.

Various spacecraft is distributed in a wide range of types of orbits, as shown in Figure 1. In MEO and HEO (M&H), various satellites are arranged near the semi-geosynchronous

The associate editor coordinating the review of this manuscript and approving it for publication was Rosario Pecora.

TABLE 1. The number of satellites in different orbits (includes launches through 11/30/18).

The earth orbit	Number
LEO	1232
MEO	126
GEO	558
The highly elliptical orbit	41

orbit and GEO. While there are more abundant spacecraft in LEO, including the International Space Station, the Hubble space telescope, and the manned spacecraft. However, countless anomalies resulted from various harsh space environment are taken place in different orbits all the time [4], [5]. To ensure the reliability of spacecraft operation in the long term, particular emphasis should be put on eliminating the main impacts of the space environment on the spacecraft in different orbits.

In this paper, a review of the space environment and its effects on spacecraft in different orbits are given. In Section 2,

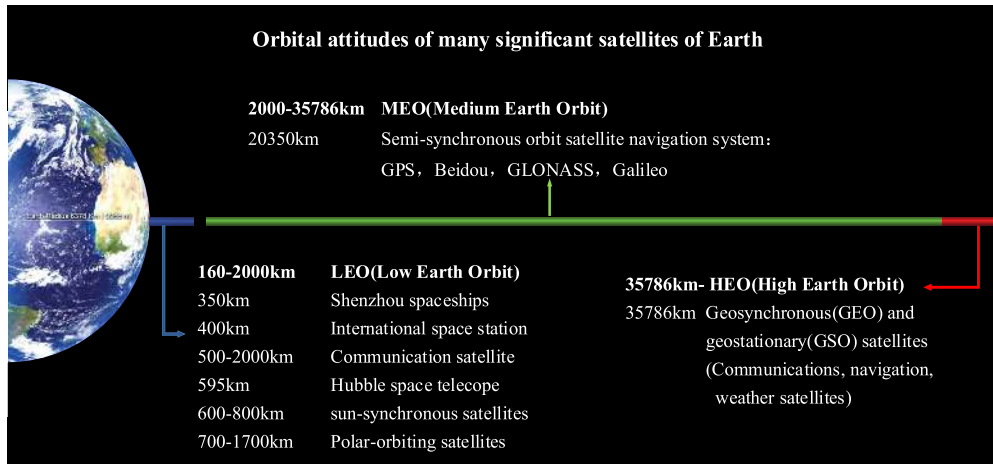


FIGURE 1. The distribution of important spacecraft in earth orbits.

the main space environment components are briefly investigated, including the neutral atmosphere, the plasma, the radiation, the macroscopic particles, the geomagnetic field, the temperature field, and solar activities. The geomagnetic field and solar activities are only discussed in Section 2, because they are usually apt to influence other environment components other than directly affect the spacecraft. In Section 3 and Section 4, the typical space environment components of LEO and M&H are classified. Specifically, the characteristics, effects on spacecraft, analyzing models, and preventing measures of these components are introduced, respectively. The unique properties of the two regions are presented by comparing the different behaviors of the same environment components.

The purpose of this paper is to provide a description of the space environment effects that need to be concerned in different orbits, and to serve as guidance for spacecraft maintenance. What should be noted is that the orbit-attitude perturbation analysis is not within the scope of this paper.

II. THE SPACE ENVIRONMENT COMPONENTS

NASA Marshall Space Flight Center describes the space environment as seven areas: the neutral atmosphere, the plasma, the radiation, meteoroids/orbital debris, thermal environment, and solar environment [6]. Since the effects of the solar environment are mainly to disturb other components, the space environment related to spacecraft operation is categorized into six areas, including the neutral atmosphere, the plasma, the radiation, the macroscopic particles [7], the geomagnetic field, and the temperature field. Different as causes and effects are, assorted environment components are intrinsically connected. When stimulated by external disturbance, a series of disturbing reactions would arise in the space.

A. THE NEUTRAL ATMOSPHERE

The neutral atmosphere includes the upper atmosphere and the gas releasing from the spacecraft surface, and the former accounts for the main part. The effects of the

neutral atmosphere consist of the atmospheric drag and the atomic oxygen effects.

As the main perturbative force in LEO, atmospheric drag has a vital influence on the shape and altitude of orbits. Nevertheless, since the orbit-attitude perturbation analysis is not the content of this paper, atmospheric drag will not be discussed in more details.

Atomic oxygen is produced by the decomposition of the neutral atmosphere under the cosmic rays. As the dominant atmosphere component in the area ranging from 200 km to 800 km, atomic oxygen accounts for 80% of the total composition in the upper atmosphere [8]. The flux of atomic oxygen is influenced by the altitude and inclination of orbits, solar cycle, geomagnetic disturbance, and seasonal cycle. Although atomic oxygen in space is far from dense, the average impact energy collided with spacecraft operating at a speed of 7-8 km/s can up to 4-5 eV [9], which is sufficient for breaking the chemical bonds of many materials. Additionally, atomic oxygen erodes the surface of materials due to its strong oxidizability. Figure 2 shows the photographs of MISSE 2 PEACE polymers before and after the exposure to atomic oxygen [10]. Moreover, the eroded organic materials would generate condensable gas volatiles, which can lead to performance degradation and contamination of optical instruments [10]–[12].



FIGURE 2. Pre-flight and post-flight photograph of the MISSE 2 PEACE polymers experiment tray [10].



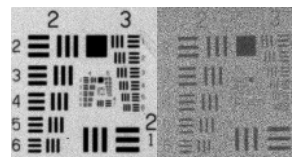
FIGURE 3. The damage of solar array caused by arcing in ESA EURECA [14].

Additionally, vacuum is another main phenomenon of the space environment, and the earth’s space is chiefly under ultra-high vacuum. In this condition, there would be adverse effects on spacecraft, such as pressure difference, discharging, out-gassing, adhesion and cold welding, materials evaporation, sublimation, and decomposition. Not only would these effects disturb other phenomena, but also bring about the loss of mass and performance, molecular pollution, and damage of instruments, etc.

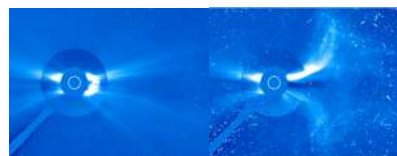
B. THE PLASMA ENVIRONMENT

The plasma is quasi-neutral to the outside, and primarily composited by electrons and ions, accounting for almost 99% in cosmic substances [13]. The manifold plasma environment in the earth’s space is made up of the ionospheric plasma, magnetospheric plasma, and solar wind plasma, which are created by the interactions among solar radiation, geomagnetic field, and the upper atmosphere. The plasma in space can be classified into hot plasma and cold plasma. Even if both of them engender surface charging, hot plasma is more threatening. The plasma generated in the earth space is mostly cold plasma, whose density and energy spectrum differ with altitude. When bombarded by the solar wind, some of the cold plasma has great chances to turn into hot plasma.

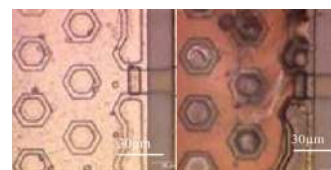
Surface charging can bring about electrostatic discharge, electromagnetic pulse jamming, solar array power loss and short circuit, material performance degradation, and accelerating contamination [14]. Figure 3 displays the burnt damage of the solar array owing to secondary discharge. On the other side, some researchers have come up with the concept that the spacecraft is defended against low-orbit spy satellites by utilizing the disturbance and destruction resulted in plasma [15]. Plentiful theoretical models are established regarding surface charging, based on satellites measurement and ground simulation [16]. The simulation for surface charging in different orbits is realized by bountiful algorithms [17]–[19]. Currently, the most versatile simulation software are NASCAP, SPIS, MUSCAT [20]. In addition to passive measures such as limiting resistivity, earthing, and electromagnetic shielding, active control of potential is also an effective way to accomplish the prevention of surface charging [21], [22].



(a) Original frames obtained by sensors with a radiation dose of 3kGy and 10kGy.



(b) CCD photographs from SOHO before and after displacement damage.



(c) Photographs of FET before and after the burnt caused by the single-event effect.

FIGURE 4. The impacts of high-energy particles [24], [26].

C. THE RADIATION ENVIRONMENT

Statistically, the anomalies caused by radiation account for approximately 40% of the total problems induced by the space environment [23]. The high-energy particles generating radiation are mainly protons, electrons, and heavy ions, which are originated from sediment in high latitude, Van Allen radiation belt, the solar cosmic ray, and the galactic cosmic ray. Since the influence of the galactic cosmic ray is much less than Van Allen radiation belt and the solar cosmic ray, it would not be taken into consideration in this paper.

Unlike the surface charging caused by plasma, high-energy particles can penetrate the surface of spacecraft, resulting in the displacement damage, internal charging, and single event effects [24]. What is more, A long-term Exposure in high-energy particles environment can lead to radiation dose damage [25]. These effects mentioned above tends to create detriments to sensitive apparatus and data processing, etc., because of problems like logic circuits flipping [26]. Figure 4 displays the disservice to sensors, charge-coupled devices (CCD), and field-effect tubes (FET) caused by radiation.

Since high-energy protons are the main cause of displacement damage and single-event effect, it is crucial to anticipate their distribution and flux by modeling and simulating. Models for high-energy protons coming from Van Allen radiation belt and solar activities are established respectively, such as AP-8 and ESP [27], [28]. And models for high-energy electrons are established as well, such as AE-8 and FLUMIC [29], [30]. They realize prediction with the help of corresponding software [31]–[33]. It is noted that models are required to be selected according to their

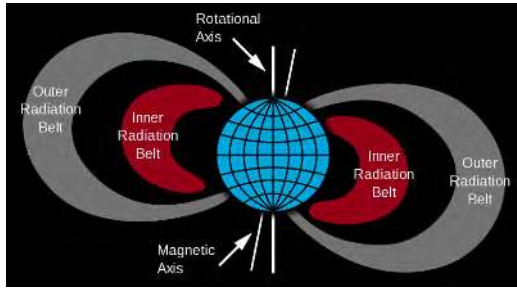


FIGURE 5. The structure of the Van Allen radiation belt [41].

applicable conditions. The spacecraft could be protected by passive measures, including satellites orbit transferring and radiation hardening technologies, and active techniques taking advantages of low-frequency radio waves, magnetic fields, and electric fields [34]–[37].

The earth's radiation belt, also known as the Van Allen radiation belt, gathers high-energy particles captured and bonded by the geomagnetic field. It consists of the inner radiation belt and the outer radiation belt, as shown in Figure 5. The inner radiation belt is the region ranging from 600 km to 10000 km, where high-energy protons predominate. Shielded by the geomagnetic field, the inner belt is barely affected by solar activities and therefore keeps stable. However, the intensity of the inner belt in low altitude lessens sharply as the altitude decreases due to the collision between particles and upper atmosphere molecules. The outer radiation belt is the region ranging from 13000 km to 45000 km, where high-energy electrons predominate. Owing to the weak protection by the geomagnetic field near the magnetopause, the high-energy electrons are susceptible to solar activities, repeating the decay-growth cycling [38]–[40].

The solar cosmic ray is the stream of high-energy particles generated by solar activities, with high intensity in a short duration. In the period of the solar flare, numerous high-energy particles, most of which are protons. And this is what we called the solar proton event. This makes the radiation environment worse, especially in M&H and polar orbits.

D. MACROSCOPIC PARTICLE ENVIRONMENT

The macroscopic particles refer to space debris and micrometeoroids. Space debris is derived from human space activities, while micrometeoroids are evolved from asteroids and comets. The impacts of both of them can bring about damage, as shown in Figure 6.

According to the size and the hazard, space debris can be categorized into three classes. Fragments larger than 10 cm in diameter are called large-sized debris, while those smaller than 1 cm in diameter are called small-sized debris. And fragments whose size are between the first two types are called medium-sized debris [42]. Though the large-sized debris can bring devastating destruction to the spacecraft, it has a low flux. Whereupon circumvention of large-sized debris should be carried out pursuant to ground-based monitoring. Not only does the small-sized debris have a high flux, but

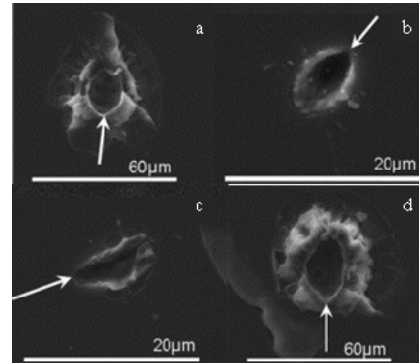


FIGURE 6. The shape of small impact: (a) and (b) space debris impacts; (c) and (d) micrometeoroid impacts. The white arrows illustrate the likely impactor trajectory [43].

also it can bring physical damage to the spacecraft, such as performance degradation of optical devices [43]. Besides, secondary destructions of internal structures and the plasma cloud forming by ultra-high-speed impacting would make the situation more troublesome. Whereupon forecasting and preventing measures are supposed to be implemented to small-sized debris pursuant to space-based monitoring [44], [45]. The medium-sized debris is difficult to be observed and therefore hard to be avoided [46]. And that is why it is classified as dangerous debris even if it has a lower flux than that of the small-sized debris. Encountering with micrometeoroids is random, and their trajectory is arduous to be detected from ground-based radars. Since the millimeter-scale micrometeoroids threaten the operation of the spacecraft, preventing measures are obliged to be applied [47]–[49].

Although space debris and micrometeoroids both would impact the spacecraft, they differ in physical properties and motion features. Space debris, with a density of 2.8 g/cm^3 , often travels in a circular orbit. Space debris usually impacts spacecraft operating in the same orbit as it does. The impact velocity is related to the inclination of orbits as well as the orientation of the spacecraft surface, and the average impact velocity of space debris is about 10 km/s. In contrast, micrometeoroids, whose density is 0.5 g/cm^3 , impact the spacecraft from all directions with an average impact velocity up to 20 km/s [50]–[52].

The number of space debris and micrometeoroids varies with the altitude of orbits, as shown in Figure 7 and Figure 8. The object count of space debris in LEO has always been accounting for a high proportion. Besides, the object count in other commonly used orbits has also risen distinctively in recent years. The flux of micrometeoroids is indicated by a combined factor which takes the earth shielding effect and gravitational convergence effect into consideration [53]. It is palpable in Figure 8 that the flux upsoars as altitudes grow in LEO, reaching the peak in the altitude about 2500 km. Contrasted with part region of M&H, the LEO is much threatened with micrometeoroids.

To keep the spacecraft out of the impact of macroscopic particles, the expert systems for forecasting and protecting

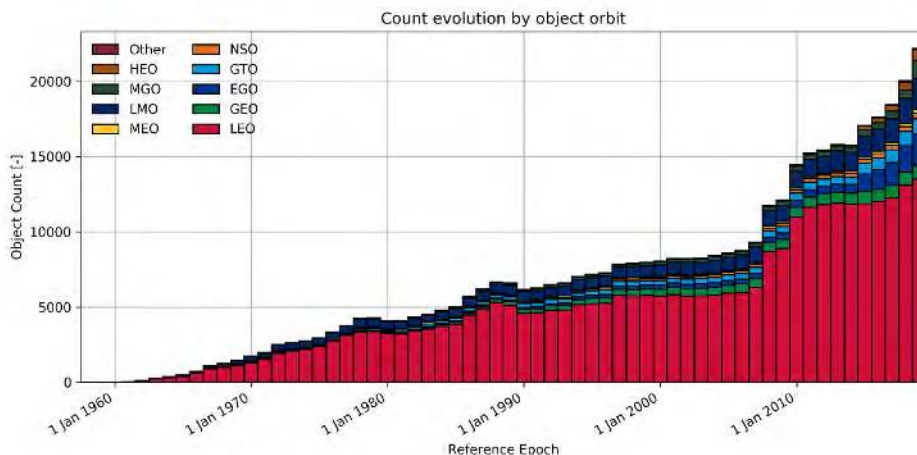


FIGURE 7. Statistics and prediction of the number of space debris in common orbit by ESA [54].

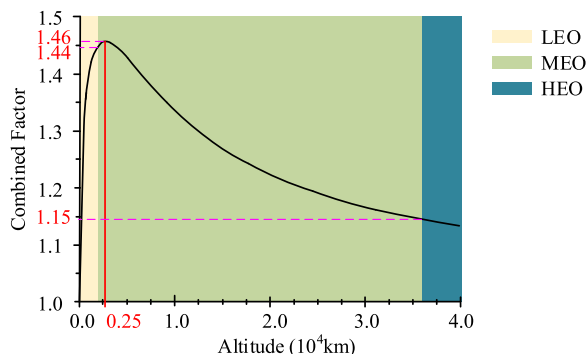


FIGURE 8. The combined factor of micrometeoroids varies with altitudes [53].

need to be established, founded on observation, modeling and simulation. By now, there has been developed plenty of observing systems and sensing methods, such as SSN and TIRA [55]. In the meanwhile, radars based on ground and space as well as optical measurements have been employed [56]. They predict the trajectories and orbits of macroscopic particles with approaches varying with altitudes and sizes [57]. Mathematical models are established for debris models, such as CODR, IDES [58], and micrometeoroid models, such as Cours-Palais, Grün, Divine-Staubach [59]–[61], as well as collision models, such as Frye, Chobotov [62], [63]. They are applied to evolution in different time span and engineering prediction for all kinds of particles. Whereupon warning procedures, such as BMBER, MDPANTO, etc., are developed, in terms of the flux, parameters, orbits, and time span of macroscopic particles [64], [65]. They are able to assess the damage, detectivities, avoidance strategies, and effectiveness of mitigation measures. Based on the experiments and simulations of impacting in an ultra-high-speed [66], [67], the protecting measures like shield structures prove to be adequate for millimeter scale macroscopic particles [68].

Due to the perturbation, the natural dying out of macroscopic particles basically depends on falling into the

TABLE 2. Statistics of space debris (up to January 2019) [80].

The size of space debris	Object count ($\times 10^4$)
>10cm	3.4
1cm~10cm	90
1mm~1cm	12800

atmosphere and burning down. In consequence, the lifespan of space debris is in connection with the altitude of orbits. Space debris in LEO can exist around decades to a hundred years, while those in M&H could remain for hundreds or even thousands of years. As stated by statistics from ESA, by the end of January 2019, the mass of all space debris in the earth’s space has exceeded 8000 tons, especially dangerous debris and large-sized debris, as shown in Table 2. Environmental management has to be carried out, otherwise, LEO would reach the state of super-critical, where the cascade collision among space objects would devastate orbit resources [69]. And therefore measures should be transferred to active removal from passive protection. At present, measures against dangerous macroscopic particles include energy dissipation, tethering, recovery, and deorbiting [70]–[72]. In various active removal techniques like capturing [73]–[75], removal by laser has an outstanding prospect of engineering application, space-based laser in particular [76]–[79], as sketched in Figure 9.

E. THE GEOMAGNETIC FIELD

The geomagnetic field ranges from the earth’s core to the magnetopause with low intensity. Since the intensity decreases outward at the speed of r^{-3} , the geomagnetic field is getting stronger as the altitude reduces. And thus LEO is the main region that the geomagnetic field has effects on [81]. Because the intensity varies with latitude in the same altitude, the geomagnetic field is relatively strong near the polar area [82]. The severe influence on the near-earth geomagnetic field comes from the solar wind, the high-speed plasma in which could induce global-scale

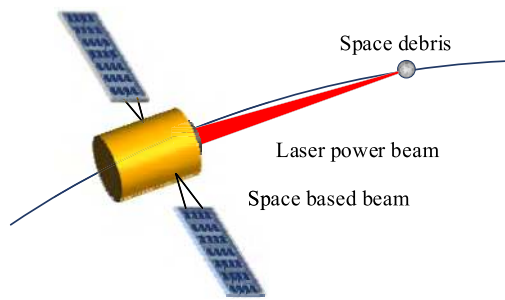


FIGURE 9. Schematic diagram of space-based laser removal of space debris.

geomagnetic storms. The geomagnetic storms would disturb the upper atmosphere and particle environment, leading to ionospheric storms and high-energy electron storms, and enhancing other adverse effects therewith [83]. Badly squeezed by the solar wind, the altitude of magnetopause diminishes from 10 Re (Re is the radius of the earth) to 3-5 Re [84]. For this reason, spacecraft in HEO and part region of MEO stands great chances to lose the shielding of the geomagnetic field completely, exposed to the harsh radiation environment of the solar wind.

As a geomagnetic field model recommended by the International Geomagnetic and Upper Air Physics Society, the International Geomagnetic Reference Field (IGRF) is an international standard for studying the geomagnetic field [85]. According to models and formulae, the intensity of the geomagnetic field at a specific time and place could be available.

F. THE TEMPERATURE FIELD

The external thermal conditions of the spacecraft in space include the solar radiation, the earth infrared, and the earth albedo, which are collectively known as space external heat, as outlined in Figure 10. While the space is equivalent to the absolute black body compared with spacecraft, acting as a heat sink. In addition, the temperature field of spacecraft is related to waste heat and circulating heat generated by itself as well. However, since the internal temperature change has little to do with the external temperature of outer parts, it can be ignored when the temperature field of outer parts is studied. In the course of periodic motion, there is mutual occlusion occurring among the spacecraft, the Earth, and the

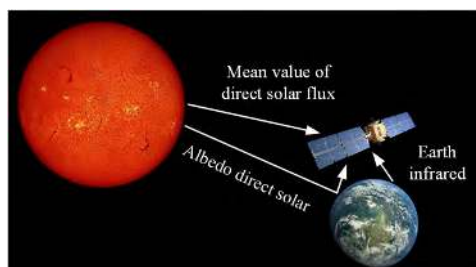


FIGURE 10. Schematic diagram of space external heat of the spacecraft.

Sun, as well as among different parts of the spacecraft. For this reason, space external heat experiences a cyclic variation. Besides, space external heat fluctuates periodically with the angle of radiation changing [86].

The ultra-high vacuum determines that thermal radiation is the primary way of heat exchange between the space environment and the spacecraft, while the interior of the spacecraft could realize heat conduction. In addition, the analysis of the temperature field is supposed to be investigated whether the occlusion is taken into consideration in terms of the thermal conduction model and radiation model. The solar radiation is stable, which occupies the main proportion of external heat. However, the intensity of the earth infrared and albedo has much to do with factors including the atmosphere, surface temperature, and time. As a result, it is hard to quantify them accurately, and simplified models have come into common usage [87], [88]. The mathematical expressions of the temperature field are established, considering the variation with orbits and operations. Whereupon, a series of procedures are developed, such as SINDA/G, I-DEAS TMG, etc. [89].

Among all the phenomena which are hostile to the spacecraft, the temperature-induced anomalies account for 11% [23]. Due to the alternate heating by space external heat and cooling by the cold black environment, the temperature of spacecraft changes dramatically, especially when entering and exiting the shadow region and the sunny region. As a consequence, the in-orbit spacecraft experiences large temperature difference and gradient, leading to thermal deformation and vibration, and bringing about anomalies like signal errors therewith. With the help of ground experiments and simulations [90], thermal control measures ought to lay stress on preventing temperature soaring distinctively and stabilizing it. Passive measures must be taken including reasonable arrangement, adoption of appropriate materials and hardware, and rational organization of heat exchange [91]. Active measures should be applied as well, including adaptive adjustment of heat exchange parameters and temperature compensation [92], [93]. However, since solar ultraviolet radiation can damage materials, thermal control facilities demand the anti-ultraviolet radiation ability [94].

G. SOLAR ACTIVITIES

The solar storm is a large-scale energy release occurring in the solar atmosphere for a short time. Energy is released in the forms of enhanced electromagnetic radiation, high-energy particles, and plasma cloud, as described in Figure 11.

The electromagnetic radiation (mainly X-ray) generated by solar storms propagates at the speed of light, taking merely 8 minutes to reach the earth and causing sudden ionospheric disturbances therewith. At that point, the amplitude and phase of the radio signal would change rapidly, leading to communication confusion between the satellite and ground. The high-energy particles spend at least dozens of minutes to reach the earth, acting directly on the spacecraft in M&H and polar orbits and causing serious radiation damage therewith. It costs the plasma cloud 1 to 3 days to reach the earth,

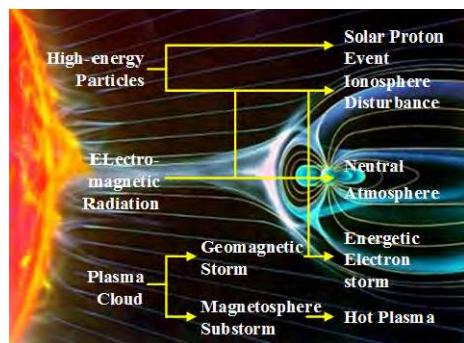


FIGURE 11. Schematic diagram of the effect of solar storms on the near-earth space environment.

inducing the global-scale geomagnetic storm. And therefore, it brings about various subsequent secondary disturbances, such as high-energy electrons storms, ionospheric storms, hot plasma injection, and the upper atmosphere densification [95]. In a nutshell, the substances and energy ejected from solar storms interact intricately with the earth's space environment, imperiling the operation of spacecraft.

H. SUMMARY

There are numerous components affecting the spacecraft, varying with altitude. In order to defend the spacecraft against those effects of phenomena efficiently, it is essential to summarize the characteristic of the space environment at a specific altitude, as outlined in Figure 12.

Except for the effects of vacuum, the gradation of colors indicates the severity of the space environment components. The vacuum effects exist continuously in the region higher than its minimum altitude. It is discernible from Figure 12 that the atomic oxygen effects and strong geomagnetic field are peculiar to LEO, while other components are altitude-varying. The ionospheric plasma and high-energy particles of the inner radiation belt maintain the upper hand in the particle environment in LEO, and the latter is primarily prevailing in the South Atlantic Anomaly and high latitude. In contrast, the particle environment in M&H consists of plasma, which comes from the geomagnetic field and solar wind, as well as high-energy particles, which come from Van Allen radiation belt and solar activities. On the other side, there are four density peaks of space debris and one flux peak of micrometeoroids in the space that spacecraft can operate. All in all, the macroscopic particle environment in LEO is much worse than that in M&H.

Figure 12 offers a quick idea about the phenomena by organizing those space environment components quantitatively by altitude. In this way, the types and severities of those components in a specific altitude are able to be consulted.

III. THE SPACE ENVIRONMENT IN LEO

LEO is a region ranging from 160 km to 2000 km. There are a series of satellites in this area, used for communication, detection [96], etc. Furthermore, LEO accommodates

various common spacecraft, such as the manned spacecraft, Hubble Space Telescope, and the International Space Station. Nevertheless, the space environment in LEO is considerably complicated. The space environment of LEO contains the neutral atmosphere, ionospheric plasma, the inner radiation belt, macroscopic particle environment, and the temperature field. Additionally, the geomagnetic field and solar activities would disturb these phenomena to varying degrees.

A. THE ATOMIC OXYGEN

The neutral atmosphere is unique to LEO, in which atomic oxygen is the principal component that detriments the spacecraft. The atomic oxygen gains a great proportion in the upper atmosphere, and is affected by many factors, as mentioned in Section 2.1. For the reason that atomic oxygen puts the spacecraft in jeopardy of denudation, erosion, and oxidation [97], lots of researches have proposed diverse theoretical models about the atomic oxygen effects [98]–[100]. Moreover, with regard to preventing measures against atomic oxygen, the most studied aspects are anti-corrosive materials and coatings [101], [102]. In the meanwhile, the results of ground experiments are not quite the same as the actual values [103]. And therefore numerical models [104], [105] and simulation technologies [106]–[108] are developed to satisfy the demands of numerical verifications.

B. THE IONOSPHERIC PLASMA

The ionosphere is the region higher than 60 km, where plasma is cold and quasi-neutral with high density and low energy. The single Maxwell distribution function is able to describe the variation of the electron density with altitude and diurnal change (see Figure 13). The ionosphere is divided into four regions in altitude named as D, E, F1, F2 according to the electron density, in which F has the densest electrons [109]. The regions in low latitude have denser electrons and more violent anomalous changes than regions in high latitude. Since the variations are connected with the earth's activities, bountiful studies have been conducted on the relations between ionospheric precursors and earthquake [110], [111].

The polar orbit is a special type of orbits in LEO, where hot plasma is sedimented in the background of dense cold plasma. As a result, the dual Maxwell function should be applied to the description of the plasma environment in polar orbits [112]. When geomagnetic field and solar activities disturb, the spacecraft passing through the polar area would be charged to negative hundreds of volts or even kilovolts.

The ionosphere is a lossy medium when transmitting radio waves. The dense electrons could enhance the attenuation of the signal [113]. Besides, the illumination of the sun has an influence on the ionosphere [114]. More severely, the solar activities could induce rapid and uneven fluctuations to the electron density, which in turn lead to the sudden ionosphere disturbances. At that time, the amplitude and phase of the radio signal which travels through the ionosphere would fluctuate fast, affecting the propagation of signals in all frequency

				Micrometeoroids			
		Space debris	800	1400	Space debris	20000	Space debris
		N40°~N50° Van Allen Inner S40°~S50° Radiation Belts		6000	13000	N40°~N50° S40°~S50°	Van Allen Outer Radiation Belts
		High-energy particles are mainly concentrated in high latitude and South Atlantic Anomaly regions		Solar Wind Plasma and Solar Cosmic Rays and Galactic Cosmic Rays			
OS	Ionospheric plasma		1000	Magnetospheric plasma			
Temperature field large temperature difference							
Stronger magnetic field intensity in LEO				Geomagnetic field			
		Atomic oxygen					
Pressure difference	Discharge	Out-gassing	Adhesion and cold welding		Materials evaporation sublimation decomposition		
Rough vacuum		High vacuum	Ultra-high vacuum	Upper atmosphere			
Sea level	100km	330km	LEO	2000km	MEO	GEO 35786km	HEO

FIGURE 12. Space environmental components in all altitudes.

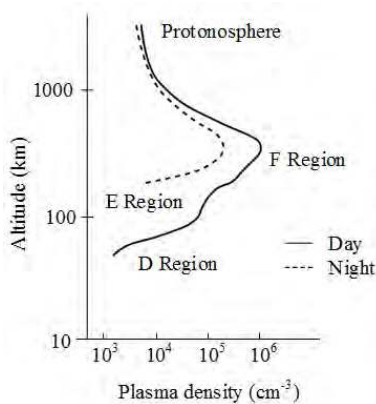


FIGURE 13. The structure of ionospheric plasma density [109].

bands, as shown in Figure 14. The severest case is communication interruption [115].

Except for communication disturbances, Ionospheric plasma charges the surface of the spacecraft as well. And hence the surface charging in LEO is bound to take space-charge effects, wake effects, and geomagnetic effects

into account [117]–[119]. And hence detection and active control measures for spacecraft in LEO are generally referred to the simulation results of the charging potential and duration.

C. THE INNER RADIATION BELT

Since LEO is located at the bottom of the inner radiation belt, the radiation environment in high latitude and South Atlantic Anomaly is tougher than other areas in LEO [120]–[122], as shown in Figure 15. The disturbances of the geomagnetic field fluctuate the properties of high-energy particles intensely with the variation of time and locations. On the other hand, although protons predominate in high-energy particles in LEO, the solar proton event has less influence on the spacecraft there owing to the shielding by the geomagnetic field.

However, the high-energy particles from solar activities could deposit in the polar regions along the magnetic lines of force. And therefore the radiation environment in polar regions is significantly affected by solar activities and the geomagnetic field. The intensity of high-energy protons there and the range of high-radiation area are positively correlated

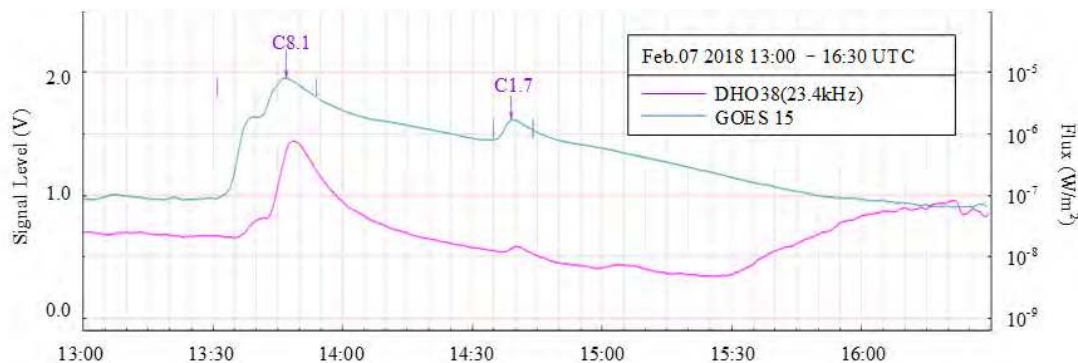
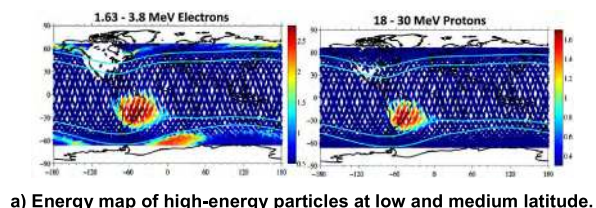
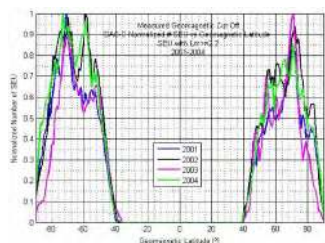


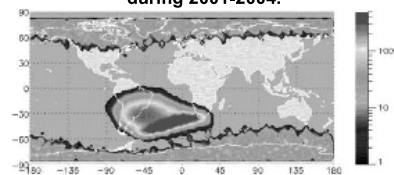
FIGURE 14. The impact of sudden ionosphere disturbances on signals on February 7, 2018 [116].



a) Energy map of high-energy particles at low and medium latitude.



b) Statistical chart of the distribution of single event effects with latitude during 2001-2004.



c) The flux of 10MeV proton during April - May 2001.

FIGURE 15. The map of high-energy particles in LEO [120]–[122].

with the intensity of solar proton events and the severity of geomagnetic storms, respectively [123]. In conclusion, the radiation environment in polar areas is much harsher than that in low latitude.

In the radiation environment of LEO, the single event effects induced by high-energy protons are the most threatening to the spacecraft. For this reason, a series of models of protons in the inner radiation belt is established for calculation and analysis, in which PSB97 and LATRM are designed for LEO [124], [125]. The flux spectrum of protons in a specific orbit could be obtained after the modification according to orbital parameters and the earth shielding effect.

D. MACROSCOPIC PARTICLE ENVIRONMENT IN LEO

The majority of the space debris is distributed in LEO, mainly concentrates in orbits with an altitude ranging from

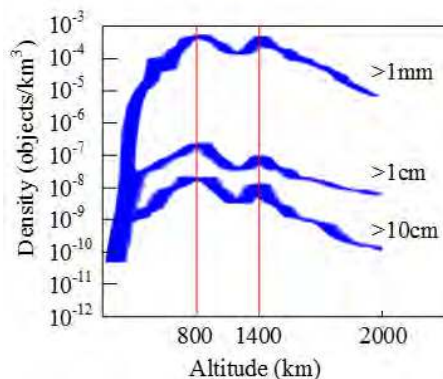


FIGURE 16. The map of high-energy particles in LEO [120]–[122].

450 km to 1200 km and an inclination ranging from 45° to 110° [126]. And there are two density peaks at the altitude of 800 km and 1400 km, respectively [127], as outlined in Figure 16. High-inclination orbits experience denser space debris in all sizes, such as polar orbits and sun-synchronous orbits. Additionally, there is a flux peak of micrometeoroids nearby the altitude of 2500 km. It is reported that the flux of millimeter micrometeoroids and space debris close by the International Space Station is virtually equivalent [52]. Numerous spacecraft in LEO is threatened by high-density macroscopic particles every now and then.

Multiples of semi-empirical models have been proposed for macroscopic particle environment in LEO, like models used for space debris, such as SDPA, CHAIN, and ORDEM, as well as models used for micrometeoroids, such as Cours-Palais [128]–[130]. Coordinating radars based on ground and space are used for monitoring, at the service of warning and prevention by expert systems mentioned before. As for the spacecraft, they require capacity for deorbiting and capturing objects. As for the management, recycling, deorbiting, and burning down are both reasonable ways, where cleaning by a space-based laser has obvious potential in engineering application [131].

E. THE TEMPERATURE FIELD IN LEO

The spacecraft in LEO is heated by solar radiation, earth infrared and earth albedo, cooled by the cold black

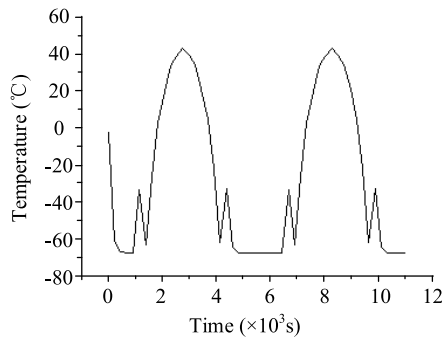


FIGURE 17. The temperature change of a feature point in an antenna in LEO [132].

environment at the same time. Because of alternate heating and cooling periodically, the spacecraft experiences a large temperature difference ranging from $-101\text{ }^{\circ}\text{C}$ to $93\text{ }^{\circ}\text{C}$ [132], as exemplified in Figure 17. Additionally, the spacecraft undergoes a dramatic gradient of temperature in the penumbra region. Since various materials are different with properties like thermal expansion coefficient, thermal deformation and vibration are inclined to happen to structures. And hence it is crucial to anticipate and control the changes of the temperature field [133].

IV. THE SPACE ENVIRONMENT IN M&H

M&H refers to a region above LEO, where MEO and HEO are separated by the GEO. With the development of satellite groups used for navigation and communication, M&H has occupied an increasingly important position. The space environment in M&H contains the plasma, radiation, macroscopic particle environment, and the temperature field, which are disturbed by geomagnetic field and solar activities to varying degrees.

A. MAGNETOSPHERIC PLASMA AND SOLAR WIND PLASMA

The plasma environment in M&H is mainly composed by magnetospheric plasma and solar wind plasma. Its particle energy spectrum is in a wide range and varies with regions [134], especially complicated in HEO. In addition to the background of cold plasma, hot plasma is frequently injected into M&H because of constant disturbance of geomagnetic storms and solar activities. As a consequence, the spacecraft in GEO could be charged to tens of thousands of volts every so often [135], as shown in Figure 18.

During the geomagnetic substorm, although the spacecraft in GEO has been severely charged in the shadow region, the charging is effectively suppressed by the photoelectron current in the sunny region [137]. The potential difference would be generated when the spacecraft is under different conditions at the same time. Additionally, the plasma also has a great impact on the transmission of signals for navigation satellites [139]. Seeing that the plasma environment in HEO is complex, the dual Maxwell distribution is applied to describe it in GEO [140]. Based on the law of surface charging

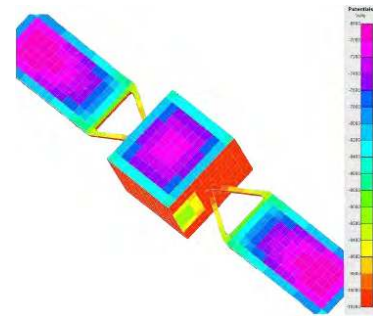


FIGURE 18. The result of stable surface charge of the spacecraft in GEO [136].

obtained by algorithms like PIC, detection and active control measures of surface potential are developed [141].

B. THE OUTER RADIATION BELT AND SOLAR PROTON EVENTS

The radiation environment in M&H mainly consists of electrons from the outer radiation belt and protons from solar proton events. A majority of navigation satellites, such as GPS and Beidou, are located at the center of the outer radiation belt, while the spacecraft in GEO is placed at the periphery of the outer radiation belt and experiences solar proton events occasionally. Moreover, the fluxes of electrons and protons near the altitude of 20000 km are both higher than that in GEO. Consequently, MEO has a more awful radiation environment than GEO during the solar minimum.

The flux of high-energy electrons in MEO varies with their intensity which is concerned with time. Seeing that the high-energy electron environment responds to geomagnetic storms nonlinearly, it is a dynamic system which changes violently [142]. The high-energy electron environment in MEO has different scales of quasi-periodic time-varying characteristics [143], while that in GEO has obvious fluctuations with local time every day and solar activities weekly [144]. The flux of high-energy electrons in GEO is negatively correlated with solar activities. During the solar minimum, its flux reaches the highest value around the spring equinox and the autumnal equinox, while it reaches the lowest value around the summer solstice and the winter solstice. It has different distributions during day and night. That is to say, it reaches the maximum at noon and the minimum at midnight in local time. Empirical models that are appropriate for M&H include AE-8, AE-9, FLUMIC, and PLOE [145], [146]. Fitted and modified by logarithmic values [147], the nonlinear correlation between high-energy electrons and solar wind or geomagnetic Ap index could be resolved by methods like neural networks [148], [149].

Since the energy and intensity of protons in the outer radiation belt are relatively low, the spacecraft orbiting higher than 24000 km is less affected by protons captured by the geomagnetic field. What they worry about more is protons derived from solar proton events. As the diminishment of the shielding effect of the geomagnetic field, the spacecraft operating in HEO suffers more severely than those operating

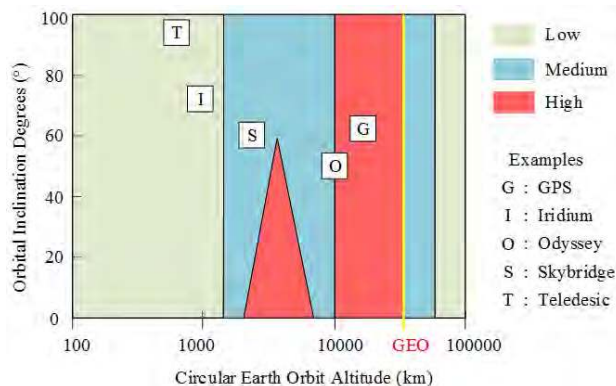


FIGURE 19. The map of internal charging risk [157].

in MEO with the same inclination. Additionally, due to the sediment of particles in polar area, the spacecraft with high inclination is more likely to be impaired by solar proton events than those with smaller inclination. Models appropriate for high-energy protons in M&H contain AP-8, CRRES PRO, TPM-1, etc., in which AP-8, AP-9, and JPL are able to apply to GEO [150], [151].

In M&H, the high-energy electrons are responsible for internal charging and total dose effects [152], while the high-energy protons are answerable for single event effects and displacement damage. According to the statistics in 2015 [153], the correlation between abnormalities of the flux of high-energy electrons and satellite anomalies was as high as 80%. Since internal charging acts as the main cause of anomalies in GEO [65], the high-energy electrons are the most threatening in the radiation environment of GEO.

Figure 19 shows the risk assessment of internal charging in different orbits given by NASA. The chart provides a quick idea about whether internal charging should be of concern in a simple way. In the meanwhile, the situations of a few common satellites are marked on it. As we can see, the internal charging is not the principal problem in LEO, while most of the spacecraft in M&H including GEO is at much higher risk. On the basis of empirical models, the internal electric field of the spacecraft can be simulated by taking advantages of software like DICTAT and SEAES [154]–[156].

C. MACROSCOPIC PARTICLE ENVIRONMENT IN M&H

The density of space debris in M&H is much less than that in LEO. Even if at the peaks of each size, it is still 1-2 orders of magnitude smaller, and the density of space debris reduced drastically in regions higher than GEO. Nevertheless, except for regions at the bottom of MEO, space debris in M&H cannot be cleared up by the atmosphere, which leads to a long lifespan and rapid increase of it. Figure 20 demonstrates that there are two density peaks around 20000 km and GEO [127]. Compared with LEO, low as the probability of collision is, space debris is still threatening for spacecraft operating around the peaks. On the other side, the flux of micrometeoroids in M&H is far from close to that

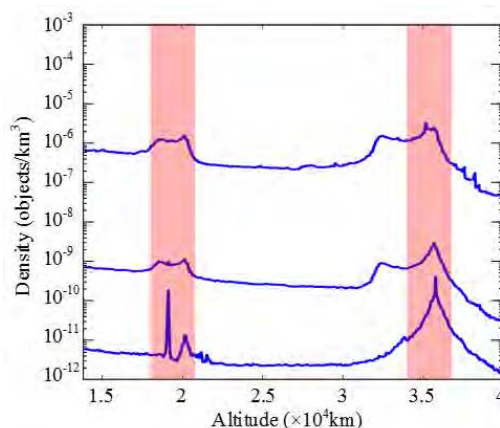


FIGURE 20. The density of space debris in M&H [127].

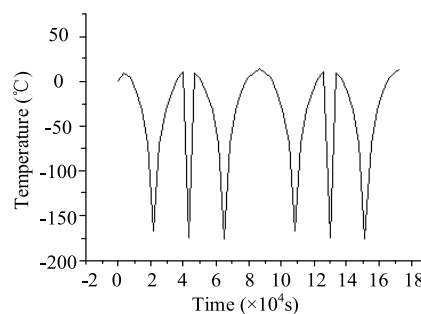


FIGURE 21. The temperature change of a feature point in an antenna in GEO [132].

in LEO, and therefore space debris the main hazard of macroscopic particle environment.

Ground-based radars have difficulties in monitoring dangerous debris in M&H accurately due to the high altitude. Whereupon, optical observation is the main approach with the guidance of efficient search strategies [158]. Multiples of semi-empirical models for M&H have been proposed, such as MASTER, LUCA, and SDM/STAT [128]–[130]. The spacecraft in M&H requires capacity for deorbiting and sending items to graveyards. Besides, capturing in-orbit should be available for space debris in specific orbit [159]–[161], to dispose of them by collecting or removing [70], [72].

D. THE TEMPERATURE FIELD IN M&H

Spacecraft in M&H suffers space external heat containing solar radiation, earth infrared, earth albedo, as well as the heat sink of cold black environment. Seeing that the effects of earth infrared and albedo are one order of magnitude smaller than that of solar radiation at least, the temperature changing could mainly consider the effects of solar radiation in some cases [162].

The temperature difference in M&H is larger than that in LEO, as exemplified in Figure 21. The maximum difference of an antenna with an aperture of 7.5 m could be up to 200 °C at the same time [163]. Large difference like this is inclined to induce thermal deformation and vibration which is harmful

to operation. However, since the spacecraft in M&H takes a longer time to pass through the penumbra region, it suffers a relatively small gradient of temperature than that in LEO.

V. CONCLUSIONS

There are distinct differences in all kinds of environmental components between LEO and M&H. The environmental components primarily considered for spacecraft in LEO contain the neutral atmosphere, ionospheric plasma, the inner radiation belt, macroscopic particle environment, the temperature field, and the geomagnetic field. Due to its low altitude, LEO is the main affected region of the upper atmosphere and the geomagnetic field, which are peculiar to LEO. The ionospheric plasma is predominant in the plasma environment in LEO, with low energy and high concentration. Most region of LEO is located at the bottom of the inner radiation belt, and South Atlantic Anomaly and polar areas are most severely affected by the radiation. Besides, macroscopic particles are densest in LEO, and threats for spacecraft with high inclination are larger than those with small inclination. Except for the large temperature difference, spacecraft in LEO suffers a great temperature gradient in the penumbra region. The polar orbit is a special type of orbits in LEO. Particles and plasma settle there and the charged particle environment is more horrible than low-latitude regions. Shielded by the geomagnetic field, LEO is less influenced by hot plasma and high-energy particles ejected by solar activities. On the other hand, due to the intense geomagnetic field, the neutral atmosphere, plasma, and radiation are sensitive to geomagnetic disturbances.

The environmental components primarily considered for spacecraft in M&H contain the plasma, radiation, macroscopic particle environment, and the temperature field. Due to weak protection of the geomagnetic field, the spacecraft in M&H is susceptible to solar activities. The plasma environment in M&H consists of magnetospheric plasma and solar wind plasma. With hot plasma injected in the background of cold plasma, the plasma environment in M&H has high energy but low concentration. Besides, the radiation environment is affected by both the Van Allen radiation belt and solar cosmic rays. During the solar minimum, the radiation in MEO is even worse than that in GEO. Additionally, sparse as macroscopic particles in M&H, the threats are serious than that in LEO, because of the limitation of macroscopic particle management conditions, HEO in particular. Moreover, compared with LEO, there is a larger temperature difference for spacecraft in M&H to suffer. However, the temperature gradient is little smaller owing to the relatively long time when passing through the penumbra area.

It can be seen that various space environmental components have different impacts on the spacecraft operation, which could lead to numerous anomalies. It is noticeable that the specific environment analysis for different orbits is the very demanding basis of spacecraft maintenance. This paper can provide technological support for the design of spacecraft in different orbits.

REFERENCES

- [1] J.-C. Liou, A. Rossi, H. Krag, M. X. J. Raj, A. K. Anilkumar, T. Hanada, and H. Lewis, "Stability of the future LEO environment," in *Proc. 6th Eur. Conf. Space Debris (ESA SP-723)*. Darmstadt, Germany: Int. Agency SpaceDebris Coordination Committee Working Group 2, Apr. 2013, pp. 22–25.
- [2] *User Support Guide: Platforms, Definitions Geocentric Orbits* Goddard Space Flight Center, NASA Goddard Space Flight Center, Greenbelt, MD, USA, 2012-07-08.
- [3] Union of Concerned Scientists. (May 2019). *UCS Satellite Database*. [Online]. Available: <https://www.ucsusa.org/nuclear-weapons/space-weapons/satellite-database>
- [4] M. Kaplan and M. Hudaverdi, "The correlations of space weather and satellite anomalies: RASAT," in *Proc. Int. Conf. Recent Adv. Space Technol.*, Jun. 2013, pp. 711–715.
- [5] H. C. Koons, J. E. Mazur, R. S. Selesnick, J. B. Blake, J. F. Fennell, and J. L. Roeder, "The impact of the space environment on space systems," in *Proc. Spacecraft Charging Conf.*, 2000, pp. 7–11.
- [6] K. Bedingeld, R. D. Leach, and M. B. Alexander, "Spacecraft system failures and anomalies attributed to the natural space environment," in *Proc. AIAA Space Programs Technol. Conf.* Huntsville, AL, USA: Nat. Aeronaut. Space Admin., 1996.
- [7] D. H. Hastings and H. Garrett, *Spacecraft–Environment Interactions*. Cambridge, U.K.: Cambridge Univ. Press, 2004.
- [8] B. A. Banks and S. K. R. Miller, "Overview of space environment effects on materials and GRC's test capabilities," in *Proc. NASA Seal/Secondary Air Syst. Workshop*. Cleveland, OH, USA: NASA Glenn Res. Center, 2006, pp. 484–505.
- [9] G. S. Arnold and D. R. Peplinski, "Reaction of high-velocity atomic oxygen with carbon," *AIAA J.*, vol. 24, no. 4, pp. 673–677, 1986.
- [10] K. K. De Groh, B. A. Banks, C. E. McCarthy, R. N. Rucker, L. M. Roberts, and L. A. Berger, "MISSE 2 PEACE polymers atomic oxygen erosion experiment on the international space station," *High Perform. Polym.*, vol. 20, nos. 4–5, pp. 388–409, 2008.
- [11] B. A. Banks, K. K. De Groh, and J. A. Backus, "Atomic oxygen erosion yield predictive tool for spacecraft polymers in low earth orbit," Tech. Rep. NASA/TM-2008-215490, E-16694, Dec. 2008.
- [12] B. A. Banks, K. K. De Groh, and S. K. Miller, "Low earth orbital atomic oxygen interactions with spacecraft materials," in *Proc. MRS Online Library Arch.*, vol. 851, 2004, pp. NN8.1-1–NN8.1-12.
- [13] E. Yigit, *Atmospheric and Space Sciences: Ionospheres and Plasma Environments* (SpringerBriefs in Earth Sciences), vol. 2. Dordrecht, The Netherlands: Springer, 2017.
- [14] G. Bonin, N. Orr, R. Zee, and J. Cain, "Solar array arcing mitigation for polar low-earth orbit spacecraft," in *Proc. 24th Annu. Conf. Small Satell.*, Logan, UT, USA, vol. 9012, Aug. 2010, 2010.
- [15] J. Yang, W. Su, G. Mao, and H. He, "On calculating effectiveness of Plasma defense against low orbit spy satellite," (in Chinese), *J. North-Western Polytech. Univ.*, vol. 23, no. 1, pp. 93–97, Feb. 2005.
- [16] M. J. Mandell, V. A. Davis, B. M. Gardner, I. G. Mikellides, D. L. Cooke, and J. Minor, "NASCAP-2K: An overview," in *Proc. 8th Spacecraft Charging Technol. Conf.*, 2004.
- [17] V. A. Davis, M. J. Mandell, D. C. Cooke, A. Wheelock, J.-C. Matéo-Vélez, J.-F. Roussel, D. Payan, M. Cho, and K. Koga, "Comparison of low earth orbit wake current collection simulations using Nascap-2k, SPIS, and MUSCAT computer codes," *IEEE Trans. Plasma Sci.*, vol. 41, no. 12, pp. 3303–3309, Dec. 2013.
- [18] J.-C. Mateo-Velez, J.-F. Roussel, V. Inguibert, M. Cho, K. Saito, and D. Payan, "SPIS and MUSCAT software comparison on LEO-like environment," *IEEE Trans. Plasma Sci.*, vol. 40, no. 2, pp. 177–182, Feb. 2012.
- [19] J. Forest, L. Eliasson, and A. Hilgers, "A new spacecraft plasma simulation software, PicUp3D/SPIS," in *Proc. 7th Spacecraft Charging Conf.*, Noordwijk, The Netherlands, vol. 476, 2001, pp. 515–520.
- [20] C. K. Birdsall and A. B. Langdon, *Plasma Physics Via Computer Simulation*. Boca Raton, FL, USA: CRC Press, 2004.
- [21] K. Torkar, R. Nakamura, M. Tajmar, C. Scharlemann, H. Jeszenszky, G. Laky, G. Fremuth, C. P. Escoubet, and K. Svenes, "Active spacecraft potential control investigation," *Space Sci. Rev.*, vol. 199, nos. 1–4, pp. 515–544, 2016.
- [22] W. Riedler, K. Torkar, F. Rüdener, M. Fehringer, A. Pedersen, R. Schmidt, R. J. L. Grard, H. Arends, B. T. Narheim, J. Troim, R. Torbert, R. C. Olsen, E. Whipple, R. Goldstein, N. Valavanoglou, and H. Zhao, "Active spacecraft potential control," *Space Sci. Rev.*, vol. 79, nos. 1–2, pp. 271–302, 1997.

- [23] Z. Sen, J. Shi, and J. L. Wang, "Satellite on-board failure statistics and analysis," *Spacecraft Eng.*, vol. 19, no. 4, p. 41, 2010.
- [24] V. Goiffon, M. Estribeau, O. Marcelot, P. Cervantes, P. Magnan, M. Gaillardin, C. Virmontois, P. Martin-Gonthier, R. Molina, F. Corbiere, S. Girard, P. Paillet, and C. Marcandella, "Radiation effects in pinned photodiode CMOS image sensors: Pixel performance degradation due to total ionizing dose," *IEEE Trans. Nucl. Sci.*, vol. 59, no. 6, pp. 2878–2887, Dec. 2012.
- [25] V. Goiffon, M. Estribeau, and O. Marcelot, "Radiation effects in pinned photodiode CMOS image sensors: Pixel performance degradation due to total ionizing dose," *IEEE Trans. Nucl. Sci.*, vol. 59, no. 6, pp. 2878–2887, Dec. 2012.
- [26] F. Miller, A. Luu, F. Prud'homme, P. Poirot, R. Gaillard, N. Buard, and T. Carrire, "Characterization of single-event burnout in power MOSFET using backside laser testing," *IEEE Trans. Nucl. Sci.*, vol. 53, no. 6, pp. 3145–3152, Dec. 2006.
- [27] D. M. Sawyer and J. I. Vette, *AP-8 Trapped Proton Environment for Solar Maximum and Solar Minimum*. Washington, DC, USA: NASA, 1976.
- [28] M. A. Xapsos, G. P. Summers, J. L. Barth, E. G. Stassinopoulos, and E. A. Burke, "Probability model for cumulative solar proton event fluences," in *Proc. 5th Eur. Conf. Radiat. Effects Compon. Syst. (RADECS)*, 1999, pp. 22–26.
- [29] J. I. Vette, *The AE-8 Trapped Electron Model Environment*. Washington, DC, USA: NASA, 1991.
- [30] D. J. Rodgers, K. A. Hunter, and G. L. Wrenn, "The FLUMIC electron environment model," in *Proc. 8th Spacecraft Charging Technol. Conf.*, Huntsville, AL, USA, Oct. 2004, pp. 1–13.
- [31] H. H. K. Tang, "SEMM-2: A new generation of single-event-effect modeling tools," *IBM J. Res. Develop.*, vol. 52, no. 3, pp. 233–244, May 2008.
- [32] R. A. Weller, M. H. Mendenhall, R. A. Reed, R. D. Schrimpf, K. M. Warren, B. D. Sierawski, and L. W. Massengill, "Monte Carlo simulation of single event effects," *IEEE Trans. Nucl. Sci.*, vol. 57, no. 4, pp. 1726–1746, Aug. 2010.
- [33] M. Raine, G. Hubert, M. Gaillardin, P. Paillet, and A. Bourmel, "Monte Carlo prediction of heavy ion induced MBU sensitivity for SOI SRAMs using radial ionization profile," *IEEE Trans. Nucl. Sci.*, vol. 58, no. 6, pp. 2607–2613, Dec. 2011.
- [34] J. W. Wilson, F. A. Cucinotta, and M. H. Kim, "Optimized shielding for space radiation protection," *Physica Medica, PM, Int. J. Devoted Appl. Phys. Med. Biol., J. Italian Assoc. Biomed. Phys. (AIFB)*, vol. 17, no. 1, p. 67, 2001.
- [35] M. Durante, "Space radiation protection: Destination mars," *Life Sci. Space Res.*, vol. 1, pp. 2–9, Apr. 2014.
- [36] C. C. Yui, G. M. Swift, C. Carmichael, R. Koga, and J. S. George, "SEU mitigation testing of Xilinx Virtex II FPGAs," in *Proc. Radiat. Effects Data Workshop*, Jul. 2003, pp. 92–97.
- [37] J. J. H. Adams, Jr., D. H. Hathaway, R. N. Grugel, J. W. Watts, T. A. Parnell, J. C. Gregory, and R. M. Gregory, "Revolutionary concepts of radiation shielding for human exploration of space," NASA Marshall Space Flight Center, Huntsville, AL, USA, Tech. Rep. NASA/TM-2005-213688, M-1133, 2005.
- [38] D. N. Baker, J. B. Blake, L. B. Callis, J. R. Cummings, D. Hovestadt, S. Kanekal, B. Klecker, R. A. Mewaldt, and R. D. Zwickl, "Relativistic electron acceleration and decay time scales in the inner and outer radiation belts: SAMPEX," *Geophys. Res. Lett.*, vol. 21, no. 6, pp. 409–412, 1994.
- [39] D. N. Baker, S. G. Kanekal, X. Li, S. P. Monk, J. Goldstein, and J. L. Burch, "An extreme distortion of the Van Allen belt arising from the 'Halloween' solar storm in 2003," *Nature*, vol. 432, no. 7019, pp. 878–881, 2004.
- [40] J. Goldstein, S. G. Kanekal, D. N. Baker, and B. R. Sandel, "Dynamic relationship between the outer radiation belt and the plasmopause during March–May 2001," *Geophys. Res. Lett.*, vol. 32, no. 15, 2005, Art. no. L15104.
- [41] EAS's Space Debris Office. (May 2019). *Analysis and Prediction[EB/OL]*. [Online]. Available: https://www.esa.int/Our_Activities/Operations/Space_Safety_Security/Space_Debris/Analysis_and_prediction
- [42] *National Research Council. Orbital Debris: A Technical Assessment*, National Academies Press, Washington, DC, USA, 1995.
- [43] A. T. Kearsley, G. Drolshagen, J. A. M. McDonnell, J.-C. Mandeville, and A. Moussi, "Impacts on hubble space telescope solar arrays: Discrimination between natural and man-made particles," *Adv. Space Res.*, vol. 35, no. 7, pp. 1254–1262, 2005.
- [44] E. L. Christiansen, "Design and performance equations for advanced meteoroid and debris shields," *Int. J. Impact Eng.*, vol. 14, nos. 1–4, pp. 145–156, 1993.
- [45] A. B. Jenkin and G. E. Peterson, "Collision risk management in geosynchronous orbit," *Adv. Space Res.*, vol. 34, no. 5, pp. 1188–1192, 2004.
- [46] J. L. Hyde, E. L. Christiansen, and J. H. Kerr, "Meteoroid and orbital debris risk mitigation in a low earth orbit satellite constellation," *Int. J. Impact Eng.*, vol. 26, nos. 1–10, pp. 345–356, 2001.
- [47] G. Drolshagen, "Hypervelocity impact effects on spacecraft," in *Proc. Conf. Meteoroids*, vol. 495, pp. 533–541, Nov. 2001.
- [48] W. J. McNeil, S. T. Lai, and E. Murad, "Charge production due to leonid meteor shower impact on spacecraft surfaces," in *Proc. 6th Spacecraft Charging Technol.*, 1998, pp. 187–191.
- [49] V. A. Chobotov and A. B. Jenkin, "Analysis of the micrometeoroid and debris hazard posed to an orbiting parabolic mirror," *Space Debris*, vol. 2, no. 1, pp. 9–40, 2000.
- [50] W. P. Schonberg, "Protecting spacecraft against meteoroid/orbital debris impact damage: An overview," *Space Debris*, vol. 1, no. 3, pp. 195–210, 1999.
- [51] G. J. Dittberner, M. L. Fudge, J. S. Huth, N. L. Johnson, and D. S. Mcknight, "Examining simplifying assumptions of probability of collisions in LEO," in *Proc. 1st Eur. Conf. Space Debris*, Darmstadt, Germany, 1993, pp. 485–489.
- [52] V. Ekstrand and G. Drolshagen, "Comparison of meteoroid and space debris fluxes to spacecraft in earth orbit," in *Proc. Meteoroids Conf.*, vol. 495, 2001, pp. 543–550.
- [53] D. J. Kessler and R. C. Reynolds, and P. D. Anz-Meador, "Space station program natural environment definition for design," Int. Space Station Alpha, Nat. Aeronaut. Space Admin. Space Station Program Office, Houston, TX, USA, Tech. Rep. NASA SSP 30425, 1994.
- [54] A. Whittlesey and H. B. Garrett, "NASA's technical handbook for avoiding on-orbit ESD anomalies due to internal charging effects," in *Proc. 6th Spacecraft Charging Technol.*, 1996, pp. 131–134.
- [55] D. Mehrholz, L. Leushacke, W. Flury, R. Jehn, H. Klinkrad, and M. Landgraf, "Detecting, tracking and imaging space debris," *ESA Bull.*, vol. 109, no. 109, pp. 128–134, 2002.
- [56] T. Schildknecht, "Optical surveys for space debris," *Astron. Astrophys. Rev.*, vol. 14, no. 1, pp. 41–111, 2007.
- [57] G. Tommei, A. Milani, and A. Rossi, "Orbit determination of space debris: Admissible regions," *Celestial Mech. Dyn. Astron.*, vol. 97, no. 4, pp. 289–304, 2007.
- [58] R. Jehn, "Comparison of the 1999 beam-park experiment results with space debris models," *Adv. Space Res.*, vol. 28, no. 9, pp. 1367–1375, 2001.
- [59] A. V. Moorhead, "Meteoroid environment modeling: The meteoroid engineering model and shower forecasting," in *Proc. Appl. Space Environ. Conf. (ASEC)*, Huntsville, AL, USA, 2017.
- [60] B. G. Cour-Palais, "NASA space vehicle design criteria-environment," Meteoroid Environ. Model-1969/Near Earth Lunar Surface, Nat. Aeronaut. Space Admin., Office Adv. Res. Technol., Washington, DC, USA, Tech. Rep. NASA SP-8013, 1969.
- [61] P. Staubach and E. Grün, "Development of an upgraded meteoroid model," *Adv. Space Res.*, vol. 16, no. 11, pp. 103–106, 1995.
- [62] J. W. Frye, "Collision probability estimate method for impact generated low earth orbit space debris clouds," *Astrodynamics*, vol. 1992, pp. 287–310, Aug. 1991.
- [63] V. A. Chobotov and D. L. Mains, "Tether satellite system collision study," *Acta Astronautica*, vol. 44, nos. 7–12, pp. 543–551, 1999.
- [64] E. L. Christiansen, K. Nagy, and J. Hyde, "Bumper 3 update for IADC protection manual," in *Proc. 34th Inter-Agency Space Debris Coordination Committee Meeting*, 2016.
- [65] H. F. Wang, Q. B. Yu, Y. Y. Liu, and H. Wang, "M/OD risk assessment system and its applications," *J. Beijing Inst. Technol.*, vol. 18, no. 1, pp. 6–10, 2009.
- [66] F. K. Schäfer, M. Herrwerth, S. J. Hiermaier, and E. E. Schneider, "Shape effects in hypervelocity impact on semi-infinite metallic targets," *Int. J. Impact Eng.*, vol. 26, nos. 1–10, pp. 699–711, 2001.
- [67] R. J. Turner, E. A. Taylor, J. A. M. McDonnell, H. Stokes, P. Marriott, J. Wilkinson, D. J. Catling, R. Vignjevic, L. Berthoud, and M. Lambert, "Cost effective honeycomb and multi-layer insulation debris shields for unmanned spacecraft," *Int. J. Impact Eng.*, vol. 26, nos. 1–10, pp. 785–796, 2001.

- [68] R. Destefanis, F. Schäfer, M. Lambert, M. Faraut, and E. Schneider, "Enhanced space debris shields for manned spacecraft," *Int. J. Impact Eng.*, vol. 29, nos. 1–10, pp. 215–226, 2003.
- [69] J.-C. Liou and N. L. Johnson, "Risks in space from orbiting debris," *Science*, vol. 311, pp. 340–341, Jan. 2006.
- [70] M. Bender, "Flexible and low-cost dragon spacecraft for orbital debris removal," in *Proc. NASA/DARPA Orbital Debris Conf.*, 2009.
- [71] R. Hoyt, "RUSTLER: Architecture and technologies for low-cost remediation of the LEO large debris population," in *Proc. NASA/DARPA Orbital Debris Conf.*, 2009. [Online]. Available: http://www.tethers.com/papers/Tethers_RUSTLER_Presentation.pdf
- [72] S. Kawamoto and Y. Ohkawa, "Strategies and technologies for cost effective removal of large sized objects," in *Proc. NASA/DARPA Orbital Debris Conf.*, 2009.
- [73] C. Bonnal, J.-M. Ruault, and M.-C. Desjean, "Active debris removal: Recent progress and current trends," *Acta Astronautica*, vol. 85, pp. 51–60, Apr./May 2013.
- [74] Z. Wang, B. Wang, L. Xu, and Q. Xie, "Feedback-added pseudoinverse-type balanced minimization scheme for kinematic control of redundant robot manipulators," *IEEE Access*, vol. 7, pp. 23806–23815, 2019.
- [75] X. Chen and S. Qin, "Kinematic modeling for a class of free-floating space robots," *IEEE Access*, vol. 5, pp. 12389–12403, 2017.
- [76] M. Vasile, C. Maddock, and C. Saunders, "Orbital debris removal with solar concentrators," in *Proc. 61st Int. Astron. Congr. (IAC)*, 2010, Paper IAC-10. A6. 4.
- [77] E. S. Smith, R. J. Sedwick, J. F. Merk, and J. McClellan, "Assessing the potential of a laser-ablation-propelled tug to remove large space debris," *J. Spacecraft Rockets*, vol. 50, no. 6, pp. 1268–1276, 2013.
- [78] C. R. Phipps, K. L. Baker, S. B. Libby, D. A. Liedahl, S. S. Olivier, L. D. Pleasance, A. Rubenchik, J. E. Trebes, E. V. George, B. Marcovici, and J. P. Reilly, "Removing orbital debris with lasers," *Adv. Space Res.*, vol. 49, no. 9, pp. 1283–1300, 2012.
- [79] C. R. Phipps, "A laser-optical system to re-enter or lower low earth orbit space debris," *Acta Astronaut.*, vol. 93, pp. 418–429, Jan. 2014.
- [80] EAS's Space Debris Office, Berlin, Germany. (May 2019). *Space Debris by the Numbers[EB/OL]*. [Online]. Available: https://www.esa.int/Our_Activities/Operations/Space_Safety_Security/Space_Debris/Space_debris_by_the_numbers
- [81] J. Sharma, B. S. Ratanpal, U. M. Pirzada, and V. Shah, "Simulation of motion of satellite under the effect of oblateness of earth and atmospheric drag," 2016, *arXiv:1610.02156*. [Online]. Available: <https://arxiv.org/abs/1610.02156>
- [82] M. Kono and P. H. Roberts, "Recent geodynamo simulations and observations of the geomagnetic field," *Rev. Geophys.*, vol. 40, no. 4, pp. 4–1–4–53, 2002.
- [83] W. D. Gonzalez, J. A. Joselyn, Y. Kamide, H. W. Kroehl, G. Rostoker, B. T. Tsurutani, and V. M. Vasylunas, "What is a geomagnetic storm?" *J. Geophys. Res.*, vol. 99, no. A4, pp. 5771–5792, 1994.
- [84] J.-H. Shue, P. Song, C. T. Russell, J. T. Steinberg, J. K. Chao, G. Zastenker, O. L. Vaisberg, S. Kokubun, H. J. Singer, T. R. Detman, and H. Kawano, "Magnetopause location under extreme solar wind conditions," *J. Geophys. Res., Space Phys.*, vol. 103, no. A8, pp. 17691–17700, 1998.
- [85] S. Macmillan and J. M. Quinn, "The 2000 revision of the joint UK/US geomagnetic field models and an IGRF 2000 candidate model," *Earth, Planets Space*, vol. 52, no. 12, pp. 1149–1162, 2000.
- [86] C.-S. Kim, Q. Li, and C.-C. J. Kuo, "Fast intra-prediction model selection for H.264 codec," *Proc. SPIE*, vol. 5241, pp. 99–111, Nov. 2003.
- [87] W. Xiaodi, H. Chaochao, L. Yongshun, L. Xiangyin, and Y. Hua, "Surface temperature and infrared feature of a satellite," *Infr. Laser Eng.*, vol. 40, no. 5, pp. 805–810, 2011.
- [88] D. Bhandari and T. Bak, "Modeling earth albedo for satellites in earth orbit," in *Proc. AIAA Guid., Navigat., Control Conf. Exhib.*, 2005, p. 6465.
- [89] P. R. Zarda, T. Anderson, and F. Baum, "FEM/SINDA: Combining the strengths of NASTRAN, SINDA, I-DEAS, and PATRAN for thermal and structural analysis," in *Proc. 21st NASTRAN (R) Users' Colloq.*, Tampa, FL, USA, 1993, pp. 41–59.
- [90] C. Liu, J. Xie, Y. Wang, B. Shen, and X. Liu, "Distributed state estimation for networked spacecraft thermal experiments over sensor networks with randomly varying transmission delays," *IEEE Access*, vol. 6, pp. 56658–56665, 2018.
- [91] S. B. Cotten, "Design, analysis, implementation, and testing of the thermal control, and attitude determination and control systems for the CanX-7 nanosatellite mission," Ph.D. dissertation, Appl. Sci. Graduate, Dept. Aerosp. Sci. Eng., Univ. Toronto, Toronto, ON, Canada, 2014.
- [92] A. A. Phoenix and E. Wilson, "Adaptive thermal conductivity metamaterials: Enabling active and passive thermal control," *J. Thermal Sci. Eng. Appl.*, vol. 10, no. 5, 2018, Art. no. 051020.
- [93] J. Liu, Y. Li, and J. Wang, "Modeling and analysis of MEMS-based cooling system for nano-satellite active thermal control," in *Proc. 2nd Int. Symp. Syst. Control Aerosp. Astronaut.*, Dec. 2008, pp. 1–6.
- [94] R. Brown and S. Cannaday, "Electron-ultraviolet radiation effects on thermal control coatings," in *Proc. 3rd Thermophys. Conf.*, 1968, p. 779.
- [95] H. Koskinen, "Space weather: From solar storms to the technical challenges of the space age," in *From the Earth's Core to Outer Space*. Berlin, Germany: Springer, 2012, pp. 265–278.
- [96] Z. Qu, G. Zhang, H. Cao, and J. Xie, "Leo satellite constellation for Internet of Things," *IEEE Access*, vol. 5, pp. 18391–18401, 2017.
- [97] M. R. Reddy, "Effect of low earth orbit atomic oxygen on spacecraft materials," *J. Mater. Sci.*, vol. 30, no. 2, pp. 281–307, 1995.
- [98] B. A. Banks, T. J. Stueber, and M. J. Norris, "Monte Carlo computational modeling of the energy dependence of atomic oxygen undercutting of protected polymers," in *Protection of Space Materials from the Space Environment*. Dordrecht, The Netherlands: Springer, 2001.
- [99] B. A. Banks, J. A. Backus, M. V. Manno, "Prediction of atomic oxygen erosion yield for spacecraft polymers," *J. Spacecraft Rockets*, vol. 48, no. 1, pp. 14–22, 2011.
- [100] C.-H. Lee and L. W. Chen, "Reactive probability of atomic oxygen with material surfaces in low earth orbit," *J. Spacecraft Rockets*, vol. 37, no. 2, pp. 252–256, 2000.
- [101] E. Miyazaki, M. Tagawa, K. Yokota, R. Yokota, Y. Kimoto, and J. Ishizawa, "Investigation into tolerance of polysiloxane-block-polyimide film against atomic oxygen," *Acta Astronautica*, vol. 66, nos. 5–6, pp. 922–928, 2010.
- [102] B. Banks, M. Mirtich, S. Rutledge, D. Swec, and H. Nahra, "Ion beam sputter-deposited thin film coatings for protection of spacecraft polymers in low earth orbit," in *Proc. 23rd Aerosp. Sci. Meeting*, 1985, p. 420.
- [103] L. Bedra, M. Rutigliano, M. Balat-Pichelin, and M. Cacciatore, "Atomic oxygen recombination on quartz at high temperature: Experiments and molecular dynamics simulation," *Langmuir*, vol. 22, no. 17, pp. 7208–7216, 2006.
- [104] Y. Liu, X. Liu, G. Li, and T. Li, "Numerical investigation on atomic oxygen undercutting of the protective polymer film using Monte Carlo approach," *Appl. Surf. Sci.*, vol. 256, no. 20, pp. 6096–6106, 2010.
- [105] A. Jing, Z. Wei, and Y. Dongsheng, "Atomic oxygen environment analysis technology for low earth orbit spacecraft," in *Proc. Prognostics Syst. Health Manage. Conf.*, Jul. 2017, pp. 1–5.
- [106] K. K. De Groh, B. A. Banks, and C. E. McCarthy, "MISSE 2 PEACE polymers atomic oxygen erosion experiment on the international space station," *High Perform. Polym.*, vol. 20, nos. 4–5, pp. 388–409, 2008.
- [107] B. A. Banks, K. K. De Groh, and J. A. Backus, "Atomic oxygen erosion yield predictive tool for spacecraft polymers in low earth orbit," Tech. Rep. NASA/TM-2008-215490, E-16694, Dec. 2008.
- [108] B. A. Banks, K. K. De Groh, and S. K. Miller, "Low earth orbital atomic oxygen interactions with spacecraft materials," in *Proc. MRS Online Library Arch.*, vol. 851, 2004, pp. NN8.1-1–NN8.1-12.
- [109] E. Yigit, *Atmospheric and Space Sciences: Ionospheres and Plasma Environments* (SpringerBriefs in Earth Sciences), vol. 2. Dordrecht, The Netherlands: Springer, 2017.
- [110] T. Cussac, M.-A. Clair, P. Ultré-Guerard, F. Buisson, G. Lassalle-Balier, M. Led, C. Elisabelar, X. Passot, and N. Rey, "The demeter microsatellite and ground segment," *Planetary Space Sci.*, vol. 54, no. 5, pp. 413–427, 2006.
- [111] T. Bleier and F. Freund, "Impending earthquakes have been sending us warning signals and people are starting to listen," *IEEE Spectr.*, vol. 12, pp. 17–21, 2005.
- [112] M. S. Gussenhoven, D. A. Hardy, F. Rich, W. J. Burke, and H.-C. Yeh, "High-level spacecraft charging in the low-altitude polar auroral environment," *J. Geophys. Res., Space Phys.*, vol. 90, no. A11, pp. 11009–11023, 1985.

- [113] K. Davies, *Ionospheric Radio*. Edison, NJ, USA: IET, 1990.
- [114] E. Yiğit, P. K. Knížová, K. Georgieva, and W. Ward, "A review of vertical coupling in the atmosphere–ionosphere system: Effects of waves, sudden stratospheric warmings, space weather, and of solar activity," *J. Atmos. Solar-Terr. Phys.*, vol. 141, pp. 1–12, Apr. 2016.
- [115] C. Xiang, "Using new material to analyze the effect of ionospheric disturbance on short-wave communication," in *Proc. 7th Int. Symp. Antennas, Propag. EM Theory*, Oct. 2006, pp. 1–3.
- [116] L. Loudet. (May 2019). *SID Monitoring Station*. [Online]. Available: <https://sidstation.loudet.org/data-en.xhtml>
- [117] Y. H. Xu, J. J. Zhou, S. G. Yu, C. J. Fu, and Q. S. Wu, "A research on effects of geomagnetics and wakes on spacecraft surface charging," *Chin. Spaceence Technol.*, no. 3, pp. 29–34, 1999.
- [118] L. W. Parker, "Potential barriers and asymmetric sheaths due to differential charging of nonconducting spacecraft," Air Force Geophys. Lab., Bedford, MA, USA, Tech. Rep. AFGL-TR-78-0045, 1978.
- [119] H. B. Garrett, "The charging of spacecraft surfaces," *Rev. Geophys. Space Phys.*, vol. 19, no. 4, pp. 577–616, Nov. 1981.
- [120] X. Li, R. S. Selesnick, D. N. Baker, A. N. Jaynes, S. G. Kanekal, Q. Schiller, L. Blum, J. Fennell, and J. B. Blake, "Upper limit on the inner radiation belt MeV electron intensity," *J. Geophys. Res., Space Phys.*, vol. 120, no. 2, pp. 1215–1228, 2015.
- [121] C. Boatella, G. Hubert, R. Ecoffet, and S. Duzellier, "ICARE on-board SAC-C: More than 8 years of SEU and MCU, analysis and prediction," *IEEE Trans. Nucl. Sci.*, vol. 57, no. 4, pp. 2000–2009, Aug. 2003.
- [122] D. Falguere, D. Boscher, T. Nuns, S. Duzellier, S. Bourdarie, R. Ecoffet, S. Barde, J. Cueto, C. Alonzo, and C. Hoffman, "In-flight observations of the radiation environment and its effects on devices in the SAC-C polar orbit," *IEEE Trans. Nucl. Sci.*, vol. 49, no. 6, pp. 2782–2787, Dec. 2002.
- [123] H. D. Voss and L. G. Smith, "Global zones of energetic particle precipitation," *J. Atmos. Terr. Phys.*, vol. 42, no. 3, pp. 227–239, 1980.
- [124] S. L. Huston and K. A. Pfitzer, "Space environment effects: Low-altitude trapped proton model," NASA, Washington, DC, USA, Tech. Rep. NASA/CR 208593, 1998.
- [125] M. S. Gussenhoven, E. G. Mullen, and D. H. Brautigam, "Near-earth radiation model deficiencies as seen on CRRES," *Adv. Space Res.*, vol. 14, no. 10, pp. 927–941, 1994.
- [126] G. A. Graham, A. T. Kearsley, M. M. Grady, I. P. Wright, A. D. Griffiths, and J. A. M. McDonnell, "Hypervelocity impacts in low earth orbit: Cosmic dust versus space debris," *Adv. Space Res.*, vol. 23, no. 1, pp. 95–100, 1999.
- [127] A. Rossi, "Population models of space debris," in *Proc. Int. Astronomical Union*, 2004, pp. 427–438.
- [128] A. Rossi, L. Anselmo, A. Cordelli, P. Farinella, and C. Pardini, "Modelling the evolution of the space debris population," *Planetary Space Sci.*, vol. 46, nos. 11–12, pp. 1583–1596, 1998.
- [129] N. Johnson, E. Christiansen, R. Reynolds, M. Matney, J.-C. Zhang, P. Eichler, and A. Jackson, "NASA/JSC orbital debris models," in *Proc. 2nd Eur. Conf. Space Debris*, vol. 393, 1997, p. 225.
- [130] M. Oswald, S. Stabroth, C. Wiedemann, P. Wegener, C. Martin, and H. Klinkrad, "Upgrade of the master model," Inst. Aerosp. Syst., Tech. Univ. Braunschweig, Eur. Space Agency, Braunschweig, Germany, Tech. Rep. 18014/03, 2006.
- [131] C. R. Phipps, "L'ADROIT—A spaceborne ultraviolet laser system for space debris clearing," *Acta Astronautica*, vol. 104, no. 1, pp. 243–255, 2014.
- [132] X. X. Cheng, *Thermal Analysis Of Space Inflatable Deployment Sclerosis Film Antenna Structures*. Shanghai, China: Shanghai Jiao Tong Univ. (in Chinese), 2011.
- [133] M. F. Storz, B. R. Bowman, M. J. I. Branson, S. J. Casali, and W. K. Tobiska, "High accuracy satellite drag model (HASDM)," *Adv. Space Res.*, vol. 36, no. 12, pp. 2497–2505, 2005.
- [134] W. R. Johnston, C. D. Lindstrom, and G. P. Ginat, "Characterization of radiation belt electron energy spectra from CRRES observations," in *Proc. AGU Fall Meeting Abstr.*, San Francisco, CA, USA, 2010, Paper #SM33C-1925.
- [135] R. C. Olsen, "Record charging events from applied technology satellite 6," *J. Spacecraft Rockets*, vol. 24, no. 4, pp. 362–366, 1987.
- [136] M. J. Mandell, V. A. Davis, D. L. Cooke, A. T. Wheelock, and C. J. Roth, "Nascap-2k spacecraft charging code overview," *IEEE Trans. Plasma Sci.*, vol. 34, no. 5, pp. 2084–2093, Oct. 2006.
- [137] M. J. Mandell, V. A. Davis, B. M. Gardner, I. G. Mikellides, D. L. Cooke, and J. Minor, "NASCAP-2K: An overview," in *Proc. 8th Spacecraft Charging Technol. Conf.* Huntsville, AL, USA: NASA Marshall Space Flight Center, 2004.
- [138] S. T. Lai and M. F. Tautz, "Aspects of spacecraft charging in sunlight," *IEEE Trans. Plasma Sci.*, vol. 34, no. 5, pp. 2053–2061, Oct. 2006.
- [139] D. S. Frankel, P. E. Nebolsine, M. G. Miller, and J. M. Glynn, "Re-entry plasma induced pseudorange and attenuation effects in a GPS simulator," *Proc. SPIE*, vol. 5420, pp. 65–75, Sep. 2004.
- [140] A. Sjogren, A. I. Eriksson, and C. M. Cully, "Simulation of potential measurements around a photoemitting spacecraft in a flowing plasma," *IEEE Trans. Plasma Sci.*, vol. 40, no. 4, pp. 1257–1261, Apr. 2012.
- [141] M. J. Patterson, T. R. Verhey, G. Soulas, and J. Zakany, "Space station cathode design, performance, and operating specifications," in *Proc. 25th Int. Electr. Propuls. Conf.*, 1998.
- [142] G. D. Reeves, D. N. Baker, R. D. Belian, J. B. Blake, T. E. Cayton, J. F. Fennell, R. H. W. Friedel, M. M. Meier, R. S. Selesnick, and H. E. Spence, "The global response of relativistic radiation belt electrons to the January 1997 magnetic cloud," *Geophys. Res. Lett.*, vol. 25, no. 17, pp. 3265–3268, 1998.
- [143] T. Obara, H. Matsumoto, K. Koga, H. Koshiishi, and T. Goka, "MDS-1 observations of highly energetic electron environment in the inner magnetosphere," *Trans. Jpn. Soc. Aeronautical Space Sci., Space Technol. Jpn.*, vol. 7, no. 26, pp. 9030–9036, 2009.
- [144] D. P. Love, D. S. Toomb, D. C. Wilkinson, and J. B. Parkinson, "Penetrating electron fluctuations associated with GEO spacecraft anomalies," *IEEE Trans. Plasma Sci.*, vol. 28, no. 6, pp. 2075–2084, Dec. 2000.
- [145] H.-S. Choi, J. Lee, K.-S. Cho, Y.-S. Kwak, I.-H. Cho, Y.-D. Park, Y.-H. Kim, D. N. Baker, G. D. Reeves, and D.-K. Lee, "Analysis of GEO spacecraft anomalies: Space weather relationships," *Space Weather*, vol. 9, no. 6, pp. 1–12, 2011.
- [146] D. M. Boscher, S. A. Bourdarie, R. H. W. Friedel, and R. D. Belian, "Model for the geostationary electron environment: POLE," *IEEE Trans. Nucl. Sci.*, vol. 50, no. 6, pp. 2278–2283, Dec. 2003.
- [147] X. Li, D. N. Baker, M. Teremin, T. E. Cayton, G. D. Reeves, R. S. Selesnick, J. B. Blake, G. Lu, S. G. Kanekal, and H. J. Singer, "Rapid enhancements of relativistic electrons deep in the magnetosphere during the May 15, 1997, magnetic storm," *J. Geophys. Res., Space Phys.*, vol. 104, no. A3, pp. 4467–4476, 1999.
- [148] M. Fukata, S. Taguchi, T. Okuzawa, and T. Obara, "Neural network prediction of relativistic electrons at geosynchronous orbit during the storm recovery phase: Effects of recurring substorms," *Annales Geophysicae*, vol. 20, no. 7, pp. 947–951, 2002.
- [149] A. G. Ling, G. P. Ginat, R. V. Hilmer, and K. L. Perry, "A neural network-based geosynchronous relativistic electron flux forecasting model," *Space Weather*, vol. 8, no. 9, pp. 1–14, 2010.
- [150] D. Heynderickx, M. Kruglanski, and V. Pierrard, "Trapped radiation environment model development," Tech. Note 5, 1998.
- [151] S. L. Huston and W. Kauffman, "Space environments and effects: Trapped proton model," NASA, Washington, DC, USA, Tech. Rep. N 2, 2002.
- [152] A. Whittlesey and H. Garrett, *Avoiding Problems Caused by Spacecraft On-Orbit Internal Charging Effects*. Washington, DC, USA: NASA, 1999.
- [153] Space Environment Prediction Center. (May 2019). *Space Environment Situation Forecast in Jun. 2017 [EB/OL]*. [Online]. Available: <http://blog.sepc.ac.cn/?p=7456&cat=11>
- [154] H. Miyake, M. Honjoh, S. Maruta, Y. Tanaka, T. Takada, K. Koga, H. Matsumoto, T. Goka, B. Dirassen, L. Levy, and D. Payan, "Space charge accumulation in polymeric materials for spacecraft irradiated electron and proton," in *Proc. Annu. Rep.-Conf. Elect. Insul. Dielectric Phenomena*, Oct. 2007, pp. 763–766.
- [155] D. J. Rodgers, K. A. Ryden, G. L. Wrenn, and L. Lévy, "Fitting of material parameters for DICTAT internal dielectric charging simulations using DICTFIT," in *Proc. Int. Symp. Mater. Space Environ.*, vol. 540, 2003, pp. 609–613.
- [156] T. P. O'Brien, "SEAES-GEO: A spacecraft environmental anomalies expert system for geosynchronous orbit," *Space Weather*, vol. 7, no. 9, pp. 1–14, 2009.
- [157] A. Whittlesey and H. B. Garrett, "NASA's technical handbook for avoiding on-orbit ESD anomalies due to internal charging effects," in *Proc. 6th Spacecraft Charging Technol., Spacecraft Charging Technol.*, 1996, pp. 1–4.

- [158] M. Oswald, H. Krag, P. Wegener, and B. Bischof, "Concept for an orbital telescope observing the debris environment in GEO," *Adv. Space Res.*, vol. 34, no. 5, pp. 1155–1159, 2004.
- [159] V. S. Aslanov and V. V. Yudin, "The motion of tethered tug-debris system with fuel residuals," *Adv. Space Res.*, vol. 56, no. 7, pp. 1493–1501, 2015.
- [160] H. Liu, Q. Zhang, L. Yang, Y. Zhu, and Y. Zhang, "Dynamics of tether-tugging reorbiting with net capture," *Sci. China Technol. Sci.*, vol. 57, no. 12, pp. 2407–2417, 2014.
- [161] J. Liu, N. Cui, F. Shen, and S. Rong, "Dynamics of robotic GEostationary orbit restorer system during deorbiting," *IEEE Aerosp. Electron. Syst. Mag.*, vol. 29, no. 11, pp. 36–42, Nov. 2014.
- [162] D. G. Gilmore and M. Bello, *Spacecraft Thermal Control Handbook*. El Segundo, CA, USA: Aerospace Corporation Press, 1994.
- [163] J. T. Farmer, D. M. Wahls, R. L. Wright, and A. L. Tahernia, "Thermal distortion analysis of an antenna-support truss in geosynchronous orbit," *J. Spacecraft Rockets*, vol. 29, no. 3, pp. 386–393, 1992.



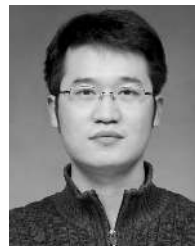
YIFAN LU was born in Harbin, Heilongjiang, in 1989. He received the B.S. and Ph.D. degrees in mechanical engineering from the Harbin Institute of Technology, in 2012 and 2018, respectively. He is currently an Assistant Professor with the Research Center of Aerospace Mechanism and Control and the State Key Laboratory of Robotics and System, Harbin Institute of Technology. His area of expertise is sensing and control of smart materials and structures. His main research interests include dynamic control of space membrane structures, precision control of shape memory alloy actuators, and novel lunar dust mitigation methods.



QI SHAO was born in Weihai, Shandong, China, in 1996. She received the B.S. degree in machine design and manufacture and automation from the Harbin Institute of Technology, Harbin, China, in 2018, where she is currently pursuing the Ph.D. degree in aerospace science and technology. She is mainly engaged in the research of active shape control of space membrane structures. Her research interests include dynamics of in-orbit gossamer spacecraft and spacecraft-environment interactions.



HONGHAO YUE born in 1978. He is currently a Professor and the Ph.D. Candidate Supervisor with the Research Center of Aerospace Mechanism Control, Harbin Institute of Technology, China. He has authored or coauthored more than 40 academic papers, which have been published in famous international journals and academic conferences. His main research interests include mechatronics engineering and active vibration control of smart structures. He has won awards, such as two national technological inventions, two first prize of Heilongjiang's technological inventions, and two awards of science and technology progress of the army.



FEI YANG was born in Yuncheng, Shanxi, in 1985. He received the B.S. degree in mechanical design and theory from Guizhou University, Guiyang, in 2007, and the M.S. and Ph.D. degrees in mechanical design and theory from the Harbin Institute of Technology, Harbin, China, in 2014. From 2014 to 2017, he was a Research Assistant with the Harbin Institute of Technology. He was promoted to Associate Professor, in 2017. His research interests include wheeled planetary vehicle mobility and space capture.

...